

Phenotypic Approaches to Identify Inhibitors of B Cell Activation

Journal of Biomolecular Screening
2015, Vol. 20(7) 876–886
© 2015 Society for Laboratory
Automation and Screening
DOI: 10.1177/1087057115585724
jbx.sagepub.com



Elizabeth B. Rex¹, Suzie Kim¹, Jake Wiener², Navin L. Rao²,
Marcos E. Milla¹, and Daniel DiSepio¹

Abstract

An EPIC label-free phenotypic platform was developed to explore B cell receptor (BCR) and CD40R-mediated B cell activation. The phenotypic assay measured the association of RL non-Hodgkin's lymphoma B cells expressing lymphocyte function-associated antigen 1 (LFA-1) to intercellular adhesion molecule 1 (ICAM-1)-coated EPIC plates. Anti-IgM (immunoglobulin M) mediated BCR activation elicited a response that was blocked by LFA-1/ICAM-1 specific inhibitors and a panel of Bruton's tyrosine kinase (BTK) inhibitors. LFA-1/ICAM-1 association was further increased on coapplication of anti-IgM and mega CD40L when compared to individual application of either. Anti-IgM, mega CD40L, or the combination of both displayed distinct kinetic profiles that were inhibited by treatment with a BTK inhibitor. We also established a FLIPR-based assay to measure B cell activation in Ramos Burkitt's lymphoma B cells and an RL cell line. Anti-IgM-mediated BCR activation elicited a robust calcium response that was inhibited by a panel of BTK inhibitors. Conversely, CD40R activation did not elicit a calcium response in the FLIPR assay. Compared to the FLIPR, the EPIC assay has the propensity to identify inhibitors of both BCR and CD40R-mediated B cell activation and may provide more pharmacological depth or novel mechanisms of action for inhibition of B cell activation.

Keywords

label free, EPIC, FLIPR, calcium flux, LFA-1/ICAM-1 adhesion

Introduction

Phenotypic screening has reemerged as a valuable approach to drug discovery. However, establishing suitable, robust screening platforms that are validated and amenable to high-throughput screening (HTS) is no trivial task. Based on a FLIPR assay developed by DiPaolo et al., we established the FLIPR-based platform to measure B cell activation to evaluate the ramifications, limitations, and differentiating attributes of the EPIC platform.¹ Our objective was to develop a label-free EPIC phenotypic platform to measure B cell activation.

The EPIC technology is label free and uses an optical biosensor that can detect changes in the index of refraction near the surface of the sensor. For cell-based assays, the dynamic mass redistribution within a cell causes index of refraction changes, resulting in a shift in the wavelength of the reflected light, and can be used to measure attachment of cells to the plate surface.² In contrast, the FLIPR-based technology uses a calcium-sensitive dye that is loaded into the cell cytoplasm. On binding of an agonist to a Gq-coupled G protein-coupled receptor, or activation of a calcium-permeable ion channel, calcium is released from intracellular stores or enters the cell via the ion channel, binds to the dye, and increases fluorescence intensity.

B cell activation is an attractive model to study due to its relevance in human health, defined signaling pathways, and repertoire of pharmacological tools that have been validated in B cell activation assays and disease models. B cell activation is dependent on two distinct signals—the first is antigen binding to the B cell receptor (BCR), followed by presentation of the antigen on the B cell surface. The second activation signal is carried out through cell-to-cell interaction between B cells and T cells. Specifically, CD40 ligand expressed on the surface of activated T cells associates with the CD40 receptor (CD40R) expressed on the surface of B

¹Discovery Sciences, Janssen Research and Development LLC, La Jolla, CA, USA

²Immunology, Janssen Research and Development LLC, La Jolla, CA, USA

Received Feb 4, 2015, and in revised form Apr 9, 2015. Accepted for publication Apr 14, 2015.

Supplementary material for this article is available on the *Journal of Biomolecular Screening* Web site at <http://jbx.sagepub.com/supplemental>.

Corresponding Author:

Elizabeth B. Rex, Discovery Sciences, Janssen Research and Development, 3210 Merryfield Row, San Diego, CA 92121, USA.
Email: erex@its.jnj.com

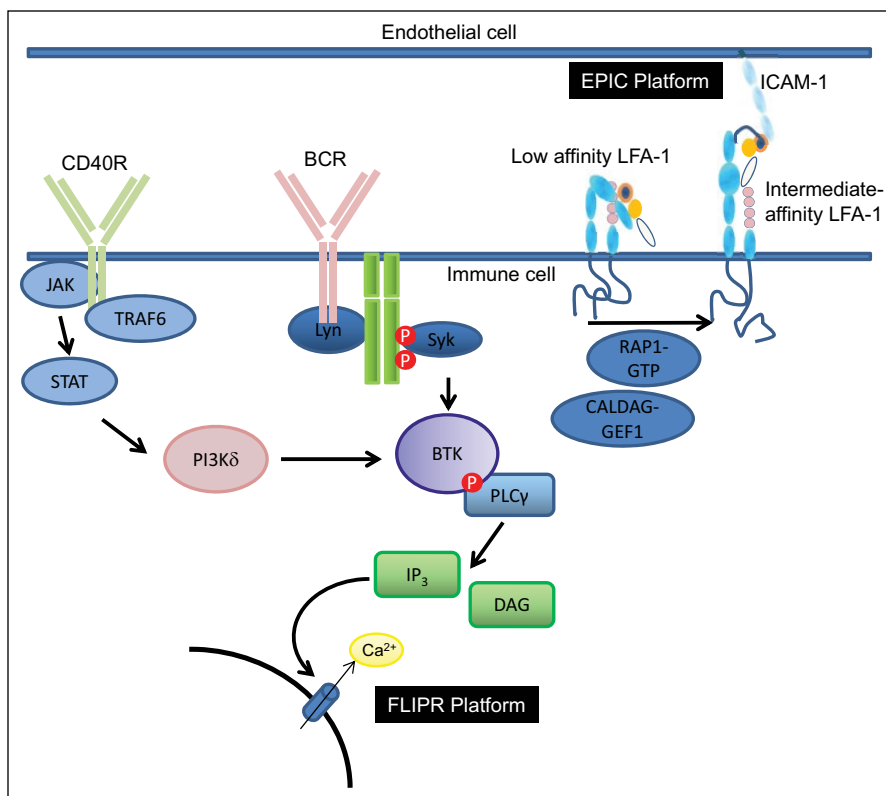


Figure 1. Signaling pathways elicited on B cell activation. Binding of antigen to the B cell receptor (BCR) results in receptor aggregation and the activation of a series of tyrosine kinases that includes lyn, spleen tyrosine kinase (syk), and Bruton's tyrosine kinase (BTK). Collectively, they form a signaling complex that activates multiple downstream effectors. The subsequent activation of phospholipase C- γ (PLC γ) catalyzes the breakdown of phosphatidylinositol 4,5 bisphosphate (PIP₂) to inositol triphosphate (IP₃) and diacylglycerol (DAG). IP₃ mediates release of Ca²⁺ from intracellular stores that is measured in the FLIPR-based technology. In parallel, DAG and Ca²⁺ activate CALDAG-GEF (Ca²⁺ and DAG guanine nucleotide exchange factor) and Rap1, which ultimately converts LFA-1 to a high-affinity conformation capable of associating with intercellular adhesion molecule 1 (ICAM-1) expressed on a target cell.⁷⁻¹⁰

cells. On activation, B cells proliferate, differentiate, and regulate antibody secretion.^{3,4} These processes are tightly regulated. Importantly, dysregulation of B cell activity contributes to the disease pathology associated with autoimmune diseases, such as systemic lupus and rheumatoid arthritis.^{5,6}

The signaling cascades elicited on B cell activation are illustrated in **Figure 1**. Briefly, engagement of BCR and/or CD40R elicits a series of signaling cascades that coalesce at the level of Bruton's tyrosine kinase (BTK). BTK is phosphorylated by kinases, such as spleen tyrosine kinase (SYK) and phosphatidylinositol-3 kinase (PI3K).^{7,8} Once activated, BTK phosphorylates and activates phospholipase C- γ (PLC γ) that gives rise to the breakdown of phosphatidylinositol 4,5 bisphosphate (PIP₂) to the second messenger's inositol triphosphate (IP₃) and diacylglycerol (DAG). IP₃ diffuses to the endoplasmic reticulum and binds to IP₃-gated calcium channels releasing Ca²⁺ into the cytoplasm. In this scenario, the FLIPR platform measures the release of calcium following BCR-dependent activation. Both DAG and Ca²⁺ activate the calcium and diacylglycerol binding guanine nucleotide exchange factor (CALDAG-GEF1). CALDAG-GEF1 is a Rap1-specific guanine nucleotide exchange factor that activates Rap1.⁹ Rap1 translocates to the membrane of B cells and, in concert with adapter proteins such as RIAM and Talins, converts low-affinity lymphocyte function-associated antigen 1 (LFA-1) to a higher-affinity conformation that is capable of associating

with cells that express intercellular adhesion molecule 1 (ICAM-1).¹⁰ ICAM-1-expressing cells include leukocytes, dendritic cells, and follicular dendritic cells.¹¹ Importantly, LFA-1/ICAM-1 protein-protein interactions are associated with the immunological synapse that forms between a lymphocyte and its target cell.¹⁰ ICAM-1 is also expressed in the membranes of endothelial cells, and, when activated, leukocytes bind to the endothelial cell via ICAM-1/LFA-1 associations and transmigrate into tissues. The EPIC assay was developed to measure the activation of B cells via the association of LFA-1-expressing B cells to EPIC plates coated with ICAM-1, a physiologically relevant response that is downstream of BCR activation and calcium release.

As mentioned previously, aberrant B cell activation is associated with autoimmune and inflammatory diseases. Identifying small-molecule inhibitors of B cell activation may ameliorate the symptoms associated with autoimmune disease. Recently, several small-molecule inhibitors of B cell activation have been reported. For example, CGI-1746 is a small-molecule BTK inhibitor that blocks BCR-dependent B cell proliferation and reduces autoantibody levels in collagen-induced arthritis.¹ Dasatinib is a small-molecule kinase inhibitor with a wide array of targets that includes SYK and BTK.^{12,13} Both SYK and BTK are downstream effectors of BCR activation (see **Fig. 1**). Indeed, dasatinib is reported to inhibit calcium release and PI3K activation in response to BCR crosslinking in chronic lymphocytic leukemia (CLL)

cells.¹³ Furthermore, dasatinib inhibits the release of histamine from human primary basophils and the secretion of pro-inflammatory cytokines in immune cells.¹² The AVL-292 class of small-molecule inhibitors is reported to inhibit B cell signaling, also via a BTK-dependent mechanism; displays efficacy in a rheumatoid arthritis model; and is currently in clinical trials.¹⁴ Small-molecule inhibitors of B cell activation that target effectors downstream of BTK and Ca^{2+} release include BMS-587101. BMS-587101 is an LFA-1 small-molecule antagonist that in vitro inhibits LFA-1-mediated adhesion of T cells to endothelial cells and blocks subsequent T cell activation.¹⁵ Importantly, BMS-587101 protects mice against inflammation and bone destruction in a collagen-induced arthritis study.¹⁵ Collectively, these data support targeting pathways involved in B cell activation for the potential treatment of autoimmune and inflammatory diseases.

In this study, we developed an EPIC-based phenotypic platform to assess B cell activation, with LFA-1/ICAM-1 adhesion being the endpoint readout. We demonstrate that the EPIC platform can detect changes in B cell adhesion to ICAM-1-coated plates triggered by stimulation of the BCR and/or CD40R. In contrast, the FLIPR assay was unable to detect CD40R-mediated changes in calcium flux under these experimental conditions. Importantly, using a series of pharmacological tools, we can block B cell activation in both the EPIC and FLIPR platforms. Whereas the FLIPR assay is truly amenable to HTS, the EPIC label-free technology provides a complementary platform that measures B cell activation from a holistic perspective. To our knowledge, this is the first report using the EPIC technology as a phenotypic screening platform to measure LFA-1/ICAM-1 adhesion as a readout for B cell activation.

Materials and Methods

Materials

The Ramos B cells and RL B cells were purchased from the American Type Culture collections (ATCC, Rockville, MD). Goat anti-IgM (immunoglobulin M) was purchased from Acris Antibodies (San Diego, CA) and Southern Biotech (Birmingham, AL). The rhICAM-1/Fc chimera and the human CD40/TNFRSF5 antibody were purchased from R & D Systems (Minneapolis, MN). Recombinant human mega CD40L was purchased from Enzo Life Sciences (Farmingdale, NY). The neutralizing anti-CD40L antibody (Anti-hCD40L-IgA) was purchased from InvivoGen (San Diego, CA). Hank's balanced salt solution (HBSS) and HEPES were purchased from Life Technologies (Grand Island, NY) and Thermo (Pittsburgh, PA), respectively. Both RPMI and PenStrep were obtained from CellGro (Corning, NY). The heat-inactivated fetal bovine serum (FBS) was purchased from PAA (Pittsburgh, PA). Black, clear-bottom, 384-well, poly D-lysine coated plates were purchased from Greiner Bio-One (Monroe, NC).

EPIC 384-well microplates were purchased from Corning (Corning, NY). The calcium assay kit was obtained from BD Biosciences (San Jose, CA). R406 and AVL-292 were made in house and can be purchased from SelleckChem (Radnor, PA). RN-486, PCI-29732, and CGI-1746 were made in house and can be purchased from MedChem Express (Monmouth Junction, NJ). Dasatinib was made in house and can be purchased from Cayman (Ann Arbor, MI). AVL-292 derivative and compound 6 were synthesized in house.¹⁶

Cell Culture

Both Ramos and RL B cells were maintained in RPMI + 10% FBS + 1× PenStrep. Cells were maintained between 5×10^5 cells/mL and 1.2×10^6 cells/mL. The day before the assays, cells were seeded in RPMI + 1% FBS + 1× PenStrep.

FLIPR Calcium Flux Assay

On the day of the assay, cells were resuspended in media containing 1% FBS, and an equal volume of the no-wash calcium dye was added to the suspension. Cells were seeded into a 384-well poly D-lysine coated plate using a Multidrop Combi (Thermo). Cells were incubated at 37°C/5% CO_2 for 1 h. For inhibition studies, cells were incubated with compound at room temperature for an additional 30 min. Compounds were diluted using the Janus Automated Workstation (Perkin Elmer, Akron, OH). Anti-IgM was prepared in HBSS supplemented with HEPES and 0.1% bovine serum albumin. Cells were stimulated with EC₈₀ anti-IgM. The change in fluorescence was recorded in the FLIPR both pre- and post anti-IgM application.

FLIPR traces were analyzed using ScreenWorks 3.2 (Molecular Devices, Grand Island, NY). The output statistic was defined as the maximum relative light units (RLUs) during the kinetic read. Data were exported to GraphPad Prism (GraphPad Prism 5 Software, San Diego, CA) for determination of IC₅₀ and EC₅₀ values

EPIC LFA-1/ICAM-1 Adhesion Assay

On the day of the assay, EPIC 5040 plates were coated with rhICAM-1 prepared in Dulbecco's phosphate buffered saline (D-PBS) at 50 ng/well. Plates were incubated at room temperature for ~3 h. Residual rhICAM-1 buffer was removed from the plates and briefly centrifuged upside down to remove remaining rh-ICAM-1 buffer. RL cells were resuspended in D-PBS and seeded in the EPIC plates at 40,000 cells/well using a Multidrop Combi. Compounds were diluted using the Janus Automated Workstation. For anti-CD40L neutralization assays, anti-CD40L was coapplied with mega CD40L. For inhibitor assays, compound was added to the EPIC plates using the Janus Automated Workstation, followed by a brief centrifugation at 300 rpm for 1 min. EPIC plates were allowed to

equilibrate in the EPIC for 2 h. Anti-IgM, mega CD40L, or CD40R antibody was prepared in D-PBS. Anti-IgM was added to the cells using the EPIC liquid-handling apparatus. A 2 min baseline read was recorded prior to anti-IgM addition, followed by a kinetic read of 2 h.

EPIC data were analyzed using the EPICAnalyzer (Corning). Time points for a given stimulus were analyzed and exported to GraphPad Prism for determination of IC_{50} and EC_{50} values. For normalized data, 100% was defined as maximal response in the absence of test compound.

Data Analysis

Figures depict representative graphs or traces. Where shown data are represented as mean \pm SD. Statistical analysis was performed with a level of significance established at $p < 0.05$. Statistical analysis was conducted using Prism software (GraphPad Prism 5).

Results

Establishing a FLIPR-Based Calcium Flux Assay to Measure B Cell Activation

A FLIPR-based assay to assess inhibitors of B cell activation has been described in the literature.^{1,17} We established the FLIPR-based platform assay in house to examine the pharmacology of a selection of tool inhibitors and compared their profiles in the EPIC platform. The Ramos and RL B cell lines were chosen to examine BCR-mediated calcium flux. Crosslinking of the BCR with anti-IgM and the subsequent activation of downstream signaling events trigger the release of calcium from intracellular stores (**Fig. 1**).^{1,17} Ramos B cells were seeded at various densities, and the calcium flux in response to anti-IgM at a range of concentrations was examined. Poly D-lysine coated 384-well plates seeded at 30,000 cells/well gave the largest response window (**Suppl. Fig. 1A**). The response peaked approximately 7 s post anti-IgM addition, followed by a slower decay (**Suppl. Fig. 1B**). To validate that the anti-IgM mediated calcium flux was signaling through the BCR signaling complex, we examined the effect of the BTK inhibitor, CGI-1746, on this system. BTK is a downstream effector of BCR signaling, and therefore inhibiting BTK should abolish intracellular calcium release (**Fig. 1**). As expected, CGI-1746 inhibited anti-IgM-mediated calcium flux in Ramos B cells in a dose-dependent fashion (**Suppl. Fig. 1C**). The potency of CGI-1746 was in the nanomolar range and consistent with published data (**Table 1**).¹

Pharmacological Characterization of Anti-IgM-Mediated Calcium Flux in Ramos B Cells

We examined the pharmacology of the tool compounds described in **Supplemental Figure 2** in the FLIPR-based

platform. Both the BCR and CD40R signaling cascades converge at BTK (**Fig. 1**). The tool compounds were chosen based on their propensity to inhibit BTK, have different modes of inhibiting BTK, and/or show efficacy in disease models. The type I inhibitors include R406, dasatinib, and PCI-29732. Type I inhibitors bind to the adenosine triphosphate (ATP) site in the catalytically active conformation but do not penetrate the allosteric pocket. R406 is a SYK and BTK inhibitor with nanomolar potencies in in vitro assays.^{16,18} R406 also has been reported to inhibit approximately 15 other kinases with less than 10-fold selectivity.¹⁹ In our cell-based FLIPR assay, R406 inhibited anti-IgM-mediated calcium flux with an IC_{50} in the micromolar range (**Fig. 2A and Table 1**). Dasatinib is a multikinase src family and BTK inhibitor.^{12,20} Dasatinib has been reported to block B cell activation on crosslinking of BCR.¹³ Of the type I inhibitors we examined, dasatinib was the most potent in both Ramos and RL cell lines with an IC_{50} of 74 nM and 234 nM, respectively (**Fig. 2A and Table 1**). PCI-29732 is a reversible inhibitor of BTK. PCI-29732 is reported to inhibit BTK in the low-nanomolar range.²¹ In the FLIPR cell-based assay, PCI-29732 attenuated anti-IgM-mediated calcium flux with an IC_{50} of ~300 nM; however, in RL cells, the IC_{50} is rightward shifted (**Fig. 2A and Table 1**).

The type 1.5 inhibitors include CGI-1746 and RN-486. Type 1.5 inhibitors also bind to the catalytically active conformation at the ATP binding site in addition to an adjacent hydrophobic pocket. CGI-1746 stabilizes the inactive non-phosphorylated conformation of BTK and is reported to display ~1000-fold selectivity over Tec and Src family kinases.¹ Similarly, RN-486 is reported to inhibit BTK in in vitro assays in the low-nanomolar range and displays a high degree of selectivity over other kinases.²² In the FLIPR cell-based assays described here, RN-486 was significantly more potent than CGI-1746 at attenuating anti-IgM-mediated calcium flux in Ramos cells (**Fig. 2B and Table 1**).

Compound 6 is a type II inhibitor.¹⁶ Type II inhibitors bind to the catalytically inactive form of the enzyme and extend into a hydrophobic allosteric site. Compound 6 is a Src family and BTK kinase inhibitor.¹⁶ Compound 6 is reported to inhibit BTK with an IC_{50} in the low-micromolar range based on a radioactive enzyme assay monitoring BTK product formation.²³ In the FLIPR cell-based assay, compound 6 did not block anti-IgM mediated calcium release in Ramos cells, even up to concentrations of 10 μ M (**Fig. 2A and Table 1**).

We selected two covalent compounds, AVL-292 and its derivative. Covalent inhibitors also form high-affinity interactions with the target enzyme, whereby the compound is irreversibly locked to the target. AVL-292 is reported to potently inhibit BTK in biochemical assays and inhibit anti-IgM-mediated BTK autophosphorylation in Ramos cells with nanomolar IC_{50} .¹⁴ In this report, AVL-292 was more potent than its derivative in Ramos cells. This was not the case for RL cells (**Fig. 2B and Table 1**).

Table 1. Summary of IC₅₀ Values for Tool Compounds Used in Each Phenotypic Platform.

Class of Inhibitor	Name	IC ₅₀ ± SD (nM) Ramos FLIPR	IC ₅₀ ± SD (nM) RL FLIPR	IC ₅₀ SD (nM) RL EPIC
Covalent	AVL-292	317, 432	>10,000	3794, 5153
Covalent	AVL-292 derivative	3583 ± 568	6960 ± 5540	2293 ± 383
Type I	R406	>10,000	2300, 3860	5394 ± 3852
Type I	Dasatinib	74 ± 57	234 ± 89	106 ± 53
Type I	PCI-29732	319 ± 13	1420, 1440	978, 1233
Type 1.5	CGI-1746	219 ± 57	746 ± 281	1198 ± 617
Type 1.5	RN-486	46 ± 25	327 ± 138	175 ± 113
Type 2 DFG out	Compound 6	>10,000	3513 ± 1254	>10,000
N/A	BMS 587101	>10,000	>10,000	23 ± 6
N/A	BIRT 377	>10,000	>10,000	460, 240

Data are IC₅₀ values from two independent experiments performed in triplicate, or mean ± standard deviation of three independent experiments performed in triplicate. Class of inhibitor represents the mechanism of action at BTK.

BTK, Bruton's tyrosine kinase; DFG, Asp-Phe-Gly; N/A, not applicable.

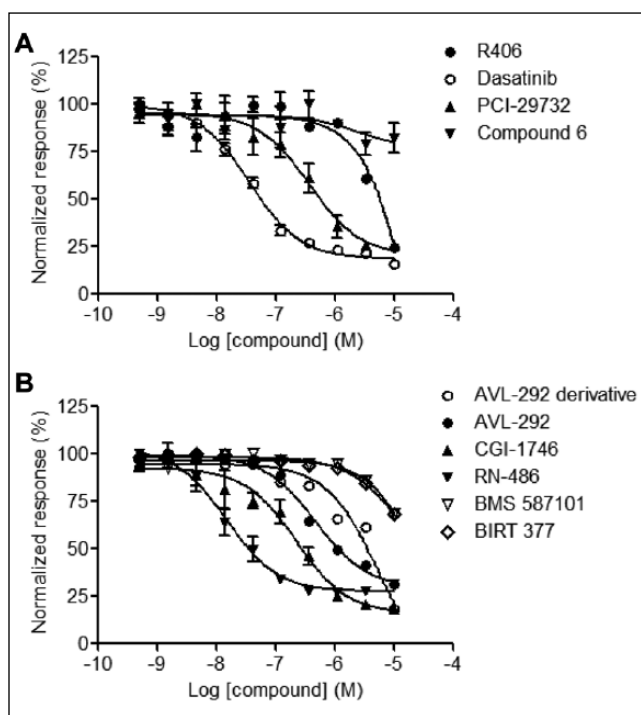


Figure 2. Pharmacological inhibition of anti-IgM (immunoglobulin M) mediated calcium flux in Ramos B cells. (A, B) Ramos B cells were incubated with compound at various concentrations prior to stimulation with anti-IgM. IC₅₀ values for the tool compounds are reported in **Table 1**. The data from representative experiments are shown as mean ± SD for each concentration performed in triplicate.

In addition to the BTK inhibitors, we also examined the propensity for LFA-1/ICAM-1 inhibitors, BMS 587101 and BIRT 377, to attenuate anti-IgM-mediated Ca²⁺ flux in the FLIPR assay. Given that Ramos B cells do not express appreciable levels of LFA-1 and that LFA-1 effector systems are downstream from Ca²⁺ flux, it was not surprising

that these inhibitors had no effect on Ca²⁺ flux (**Fig. 2B and Table 1**).²⁴ Moreover, both LFA inhibitors had no effect on Ca²⁺ flux in RL cells, further supporting that LFA-1/ICAM association occurs downstream of Ca²⁺ flux.

From a routine-profiling perspective, the FLIPR-based calcium flux platform yielded robust Z' statistics based on DMSO versus CGI-1746 (10 μM) treated cells. The average Z' was 0.75±0.03, and the Z' range was 0.69–0.79. The signal-background (s:b) was 13.4±1.5, the s:b range was 11.5–14.9.

Development of a Label-Free Platform to Measure B Cell Activation

As mentioned, RL is a human non-Hodgkin's lymphoma B cell line. RL cells express the integrin LFA-1, and association with its ligand ICAM-1 mediates B cell adhesion. The propensity for LFA-1 to associate with ICAM-1 is largely dependent on the conversion of LFA-1 to an intermediate-affinity conformation (**Fig. 1**).¹⁰ The signaling cascades elicited on BCR activation contribute to the conformational shift required for LFA-1/ICAM-1 interactions. The principle of the EPIC platform is based on association of LFA-1 expressing RL cells to ICAM-1 coated on the EPIC plate (**Suppl. Fig. 3**). We hypothesized that treatment of RL cells with anti-IgM should shift LFA-1 expressed in RL cells to an intermediate conformation capable of associating with ICAM-1 rendered on the EPIC plate. Treatment of RL cells with inhibitors of the BCR signaling pathway should abrogate the LFA-1/ICAM-1 association (**Suppl. Fig. 3**). RL cells were seeded onto 384-well EPIC plates precoated with or without ICAM-1 and allowed to equilibrate for approximately 2 h in the EPIC. The equilibration time permitted the cells to settle, resulting in a steady-state baseline. Addition of anti-IgM elicited a positive shift in response that corresponded to an increased mass within the sensing volume in

wells coated with ICAM-1 (**Fig. 3A**). The peak response was approximately 25 min post anti-IgM application, followed by a slow decay (**Fig. 3A**). The slow decay and decreased mass within the sensing volume would suggest the possible release of RL cells from the ICAM-1-coated surface. From a functional perspective, this would be consistent with immune cell extravasation and endothelial migration. Indeed, the erythromyeloblastoid leukemia cell line, K562, is reported to display dynamic LFA-1/ICAM-1 adhesion whereby a time-dependent decrease in adhesion strengthening that facilitates extravasation and transmigration was observed.²⁵ Importantly, RL cells did not appear to associate with the EPIC plate in the absence of ICAM-1, supporting the notion that the adhesion was LFA-1/ICAM-1 specific (**Fig. 3A**).

Pharmacological Characterization of the LFA-1/ICAM-1 Association

To better understand the parameters of the EPIC assay, we titrated the anti-IgM-dependent response. The anti-IgM response was dose dependent with an apparent EC_{50} of 0.9 $\mu\text{g}/\text{mL}$ (**Fig. 3B**). Data were taken at the 25–35 min time interval, at which maximal peak response was recorded. To further validate the platform, we examined the pharmacology of two well-characterized LFA-1/ICAM-1 inhibitors, BMS 587101 and BIRT 377. BMS 587101 has been shown to inhibit LFA-1-mediated adhesion of T cells to endothelial cells with an IC_{50} of 20 nM.¹⁵ Moreover, BMS 587101 is reported to be selective to LFA-1 compared to other blood-specific integrins.¹⁵ Similarly, BIRT 377 is reported to selectively inhibit LFA-1/ICAM-1 binding events in vitro and in vivo.²⁶ Importantly, in the current experiments, both BMS 587101 and BIRT 377 potently inhibited anti-IgM-mediated LFA-1/ICAM adhesion with IC_{50} s of 23 nM and 332 nM, respectively (**Fig. 3C**). In contrast, BMS 587101 and BIRT 377 did not inhibit anti-IgM-mediated Ca^{2+} flux in the FLIPR assay in either the Ramos or RL cells (**Fig. 2B and Table 1**). These data support the application of the EPIC platform for identifying inhibitors of LFA-1/ICAM association in response to anti-IgM stimulation of RL cells.

We next examined the pharmacology of the tool compounds validated in the FLIPR platform (**Suppl. Fig. 2**). In general, the potency of the compounds was consistent within the RL cell line, irrespective of assay platform. RN-486 and dasatinib were most potent at inhibiting LFA-1/ICAM adhesion (**Fig. 4A**). Similarly, these compounds were most potent at inhibiting anti-IgM-mediated calcium flux in the FLIPR assay (**Table 1**). The syk/BTK inhibitor R406 displayed potency in the micromolar range in both the FLIPR and EPIC assays. The type II inhibitor, compound 6, displayed little inhibition in both cell-based assays. Also, the covalent inhibitor, AVL-292, was an order of magnitude more potent at inhibiting anti-IgM-mediated calcium flux in Ramos cells when compared to RL cells in either platform.

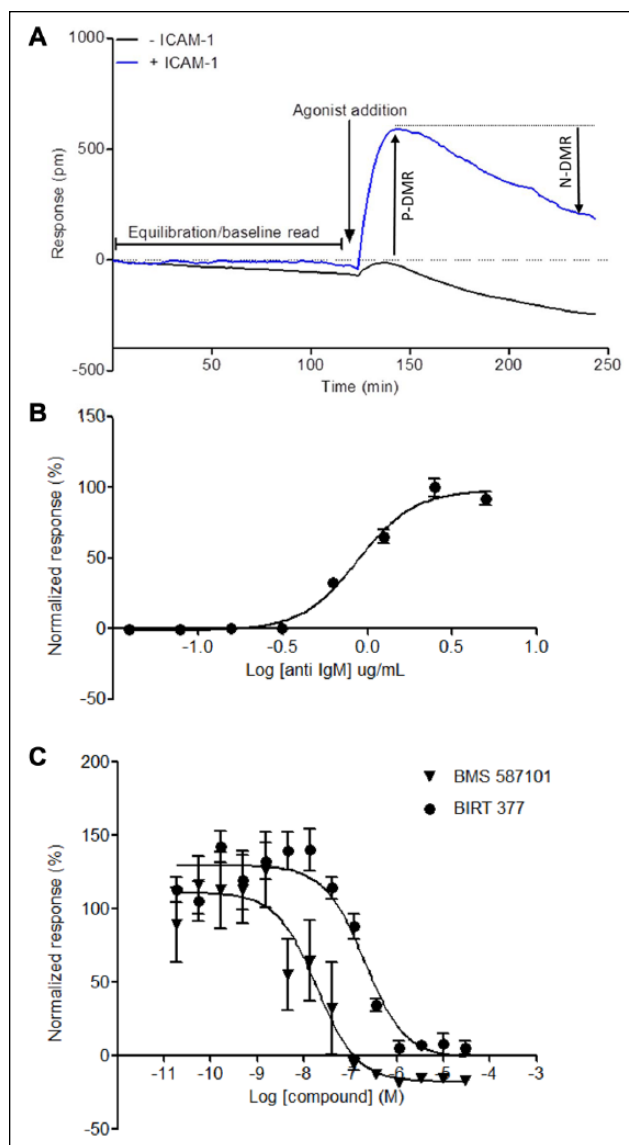


Figure 3. EPIC kinetic trace of RL cells stimulated with anti-IgM (immunoglobulin M). **(A)** RL cells were seeded on EPIC plates coated with intercellular adhesion molecule I (ICAM-I; blue trace) or uncoated (red trace). RL cells were equilibrated for approximately 2 h, followed by stimulation with anti-IgM. In the presence of ICAM-I, addition of anti-IgM increased the mass within the sensing volume representing association of RL cells to the EPIC plate. This was absent in wells not coated with ICAM-I. Following the steady-state transition, the mass slowly decreased, a response that corresponds to the RL cells dissociating from the ICAM-I-coated surface. N-DMR; negative dynamic mass redistribution (decreased mass within the cell-sensing volume); P-DMR, positive dynamic mass redistribution (increased mass within the sensing volume). **(B)** Anti-IgM titrations were performed on RL cells. The EC_{50} was 0.9 $\mu\text{g}/\text{mL}$. **(C)** Dose-dependent inhibition of anti-IgM mediated lymphocyte function-associated antigen 1 (LFA-1)-ICAM-1 association in RL cells treated with the ICAM-1/LFA-1 tool compounds, BMS 587101 and BIRT 377. Cells were incubated with compound during the 2 h equilibration period, followed by anti-IgM stimulation at EC_{90} . The IC_{50} value for BMS 587101 and BIRT 377 was 19 nM and 205 nM, respectively. The data from representative experiments are shown as mean \pm SD for each concentration performed in triplicate.

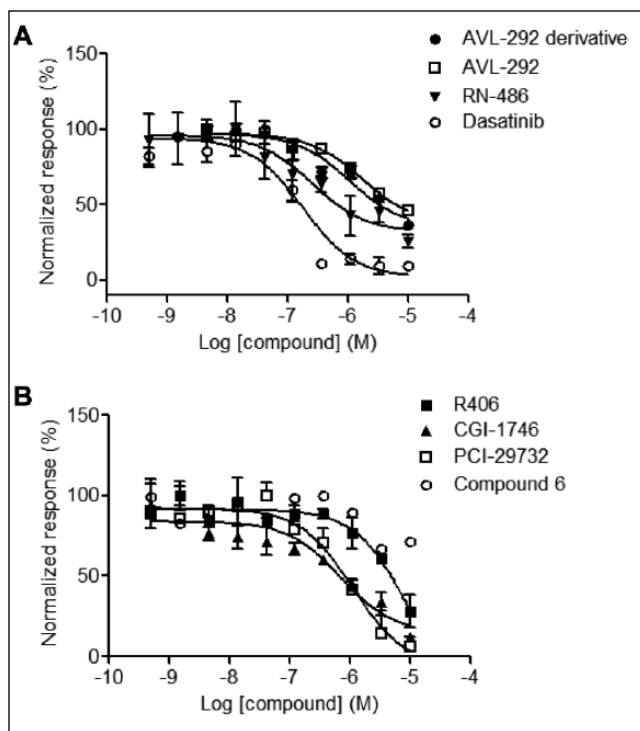


Figure 4. Pharmacological inhibition of anti-IgM (immunoglobulin M) mediated lymphocyte function-associated antigen 1 (LFA-1)/intercellular adhesion molecule 1 (ICAM-1) association in RL B cells. (**A**, **B**) RL B cells were incubated with compound at various concentrations prior to stimulation with anti-IgM. Responses were taken between 20 and 30 min post anti-IgM stimulation. IC_{50} values for the tool compounds are reported in **Table 1**. The data from representative experiments are shown as mean \pm SD for each concentration performed in triplicate.

This was not the case for the AVL-292 derivative, for which the potency of inhibition was in the micromolar range for both cell-based assays (**Table 1**).

From a routine profiling perspective, the EPIC platform yielded Z' statistics of 0.48 ± 0.05 , and the Z' range was 0.40–0.51 based on cells treated with AVL-292 (30 μ M). The s:b was 17 ± 7 , and the range was 11.5–14.9.

CD40R-Mediated LFA-1/ICAM-1 Adhesion in RL Cells

The CD40R signaling pathway activates BTK via a series of phosphorylation cascades (**Fig. 1**). Based on the simplified signaling cascade illustrated in **Figure 1**, activation of CD40R should mediate LFA-1/ICAM-1 adhesion in RL cells. We examined the effects of mega CD40 ligand (mega CD40L) and crosslinking CD40R with anti-CD40 on LFA-1/ICAM-1 adhesion. Indeed, both mega CD40L and anti-CD40R elicited LFA-1/ICAM-1 adhesion in the EPIC assay (**Fig. 5A**). However, the profile of the kinetic response was

quite different between the two stimuli. Notably, the mega CD40L dose response was maximal at 120 min post application (**Fig. 5A**). In contrast, the anti-CD40R dose response peaked between 23 and 35 min post application, followed by a slow decay (**Fig. 5A**). To confirm that the mega CD40L response was specific versus off-target effects, RL cells were cotreated with mega CD40L and mega CD40L neutralizing antibody. Importantly, the neutralizing antibody completely blocked the mega CD40L-dependent EPIC response (**Suppl. Fig. 4**). The time response for anti-CD40R is similar to that for anti-IgM-mediated LFA-1/ICAM-1 adhesion. The EC_{50} s for mega CD40L and anti-CD40 were 5 μ g/mL and 14 μ g/mL, respectively (**Suppl. Fig. 5**).

BCR and CD40R Costimulation in the EPIC and FLIPR Platforms

We hypothesized that costimulation of the BCR and CD40R signaling pathways may potentiate LFA-1/ICAM-1 adhesion in the EPIC and calcium flux in the FLIPR platform. Indeed, coapplication of anti-IgM and mega CD40L at their EC_{50} concentrations potentiated RL cell adhesion in the EPIC assay when compared to a single application of either stimulant (**Suppl. Fig. 6**). The increase of LFA-1/ICAM-1 adhesion appeared additive.

In FLIPR-based assays, activation of the CD40R with either mega CD40L or anti-CD40R did not elicit calcium flux in Ramos cells or RL cells (**Suppl. Fig. 7**). Coapplication of anti-CD40R with anti-IgM did not further increase calcium flux compared to Ramos cells treated with anti-IgM alone. Moreover, coapplication of mega CD40L/anti-IgM appeared to decrease maximal calcium flux when compared to treatment with anti-IgM alone in the Ramos cells (**Suppl. Fig. 7**).

Pharmacological Inhibition of BCR and CD40R Costimulation in the EPIC Platform

Based on our understanding of BCR and CD40R signaling, we hypothesized that a BTK inhibitor should block both the anti-IgM- and CD40R-mediated LFA-1/ICAM-1 adhesion in the EPIC assay. RL cells were treated with 10 μ M of AVL-292 or its derivative during the 2-h equilibration period followed by anti-IgM, mega CD40L, or anti-IgM/mega CD40L application at their EC_{50} concentrations. For all three conditions, treatment with the BTK inhibitors attenuated the LFA-1/ICAM-1 adhesion, although to different extents (**Fig. 5B–D**). Analysis of the kinetic traces revealed some interesting kinetic profiles. As mentioned, application of anti-IgM elicited a response within the first 25 min, followed by a slow decay (**Fig. 5B**, blue trace). Pretreatment of RL cells with AVL-292 or its derivative appeared to abolish the maximal response elicited by

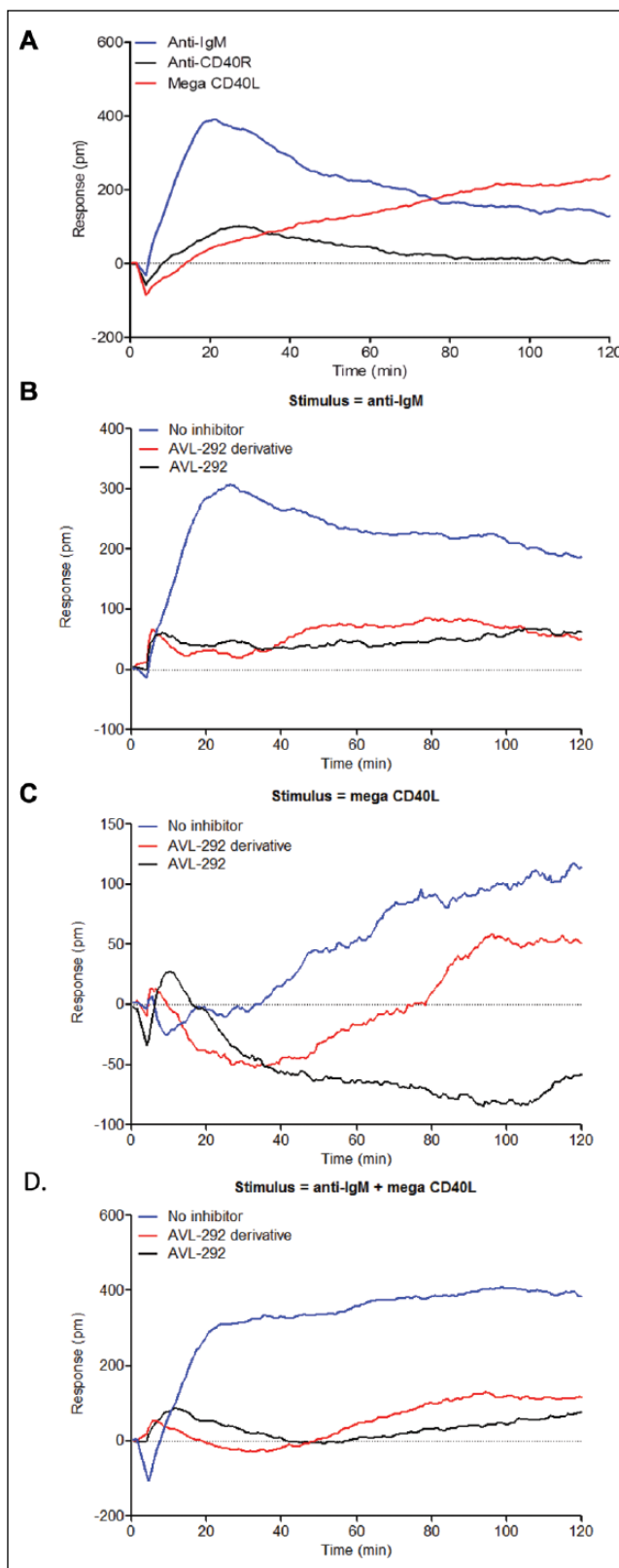


Figure 5. Pharmacological inhibition of B cell receptor (BCR)- and CD40R-mediated lymphocyte function-associated antigen 1 (LFA-1)/intercellular adhesion molecule 1 (ICAM-1) association

using the EPIC platform. **(A)** RL B cells were treated with mega CD40L, anti-CD40R, or anti-IgM (immunoglobulin M). LFA-1/ICAM-1 association was measured throughout time using the EPIC platform. Maximal response was measured 120 min post-mega CD40L stimulation. **(B–D)** RL B cells were incubated with AVL-292 or its derivative during the 2-h equilibration period followed by stimulation with the following: **(B)** anti-IgM; **(C)** mega CD40L; and **(D)** anti-IgM + mega CD40L. Blue trace: DMSO control; red trace: AVL-292 derivative (10 μ M); black trace: AVL-292 (10 μ M).

anti-IgM throughout the entire kinetic read (**Fig. 5B**, red and black traces). Application of mega CD40L displayed a slow increase in response that reached maximum at approximately 120 min post application (**Fig. 5C**, blue trace). AVL-292 pretreatment abolished the mega CD40L-dependent response up to 120 min post mega CD40L application. The AVL-292 derivative also inhibited mega CD40L-dependent LFA-1/ICAM-1 adhesion; however, the time course for the inhibition was distinct from that of AVL-292. At 30 min post mega CD40L application, the kinetic trace of the AVL-292 derivative shifted to an upward trend that parallels mega CD40L treatment alone and is characteristic of an increase in LFA-1/ICAM adhesion (**Fig. 5C**, red trace). In addition, coapplication of anti-IgM/mega CD40L yielded a kinetic trace that appeared to be a combination of the single applications of anti-IgM or mega CD40L: a robust response within the first 20–25 min followed by a slower potentiation (**Fig. 5D**, blue trace). Pretreatment of cells with either AVL-292 or its derivative inhibited the response during the first 50 min of treatment with anti-IgM + mega CD40L. The inhibition appeared to wane post 50 min, and there was a slow and steady increase in LFA-1/ICAM-1 adhesion during the remainder of the kinetic read (**Fig. 5D**, red and black traces). However, at no point during the kinetic read did the level of LFA-1/ICAM-1 association return to the response recorded in the absence of inhibitor.

Discussion

In this report, we describe the development and validation of a phenotypic, cell-based screening platform using the EPIC technology to identify inhibitors of B cell activation. We chose B cell activation as our phenotypic endpoint based on the known biology associated with B cell activation, the selection of commercially available pharmacological tools, and, importantly, the unmet medical need to find small molecules that alleviate aberrant B cell activation associated with human disease.

A revival of phenotypic, cell-based screening has occurred during the past couple of years. Indeed, a FLIPR-based B cell activation assay has been described.¹ We sought to compare and contrast both the EPIC and FLIPR

phenotypic platforms with a focus on pharmacology, throughput, and scope of the biological question.

The EPIC assay measures the propensity of RL B cells to adhere to ICAM-1-coated plates, a response that is dependent on B cells expressing LFA-1 in an “active” conformation on the surface of B cells. Association of LFA-1 to ICAM-1 is concomitant with B cell activation. The FLIPR assay measures the flux of intracellular calcium, a response that is upstream of LFA-1/ICAM-1 adhesion.

The objective of this report was to compare the scope and value of each technology as a screening platform. Ramos cells treated with anti-IgM elicited a robust Ca^{2+} response in the FLIPR assay. It is noteworthy that chronic anti-IgM treatment (on the order of 24–48 h) has been shown to elicit cell death.²⁷ Importantly, acute application of anti-IgM in these studies (2 min application) elicited a calcium response that peaked 80–100 s post application followed by decay of the signal, a kinetic profile that is not consistent with cell death. In contrast to the FLIPR assay, Ramos cells did not elicit an EPIC response, precluding their use in EPIC studies. The absence of an EPIC response in Ramos cells is likely attributed to the lack of LFA-1 expression in this cell line.²⁴ However, RL cells elicited responses in both the FLIPR and EPIC platforms.

Both the EPIC and FLIPR platforms were validated using a panel of tool compounds that have been reported to inhibit key signaling proteins and pathways involved in B cell activation and/or displayed efficacy in models of immune and inflammatory disease. In general, the rank order of potency for the tool compounds was similar for both platforms. However, there were noticeable rightward shifts in potencies for some of the compounds that were cell line dependent. The potency of the tool compounds was consistent within the RL cellular background, irrespective of assay platform. In contrast, the pharmacology generally appears to be rightward shifted when comparing Ramos cells versus RL cells in the FLIPR platform. One can speculate that the potency of a compound will depend on the cellular repertoire and possible polypharmacology within a given cell line. Indeed, the data emphasize the importance of thoroughly evaluating the cell line of choice.

With respect to potency, dasatinib and RN-486 were the only small molecules that displayed submicromolar potencies among all three cell-based assays. The type I inhibitor, R406, targets SYK and to a lesser extent BTK. R406 did not display appreciable inhibition of anti-IgM-mediated B cell activation as measured by the FLIPR and EPIC assays. R406 has been reported to block SYK-dependent BCR-mediated activation of B lymphocytes and inhibit paw inflammation in antibody-induced arthritis mouse models.¹⁸ It is worth noting that the cell-based assay used primary human B cells stimulated with anti-IgM and measured CD69 upregulation. In this scenario, cells were treated with inhibitor for 60 min followed by chronic treatment (6 h)

with anti-IgM.¹⁸ In the FLIPR-based assay, cells were treated with R406 for 30 min followed by addition of anti-IgM (acute treatment), and immediate changes in calcium flux were recorded. In the EPIC assay, RL cells were treated for 2 h with inhibitor followed by the addition of anti-IgM, and the kinetic response was recorded during a 2-h period. The apparent difference in potency of R406 may depend on the design of the assay, the final readout, and the anticipated target. Although the FLIPR and EPIC assays are phenotypic in nature and anticipated to identify inhibitors of multiple targets within the B cell activation pathway, the current experimental design is not optimized for the identification of SYK-specific inhibitors. The type 2 inhibitor, compound 6, failed to attenuate anti-IgM mediated B cell activation in the Ramos FLIPR assay and RL EPIC assay with an IC_{50} greater than 10 μM in both assay platforms. However, the potency in the RL FLIPR assay was more consistent with published data (IC_{50} of 3.5 μM versus 5.6 μM).¹⁶

As mentioned, many of these compounds have shown efficacy in animal models of inflammation and/or immune suppression. For example, CGI-1746, RN486, AVL-292, and R406 suppressed immune response in rodent models of arthritis.^{1,14,18,22} Dasatinib was reported to inhibit histamine release in primary human basophils and secretion of proinflammatory cytokines in immune cells.¹² Furthermore, in human $\text{CD}20^+$ B cells stimulated at BCR, PCI-29732 blocked the transcriptional upregulation of genes associated with B cell activation.²¹ AVL-292, dasatinib, and R406 are currently in clinical trials. AVL-292 is in Phase Ib clinical trials for the treatment of CLL, B cell non-Hodgkin's lymphoma, and Waldenström macroglobulinemia. Dasatinib combination treatment is in Phase II clinical trials for the treatment of relapsed/refractory CLL and small lymphocytic lymphoma.²⁸ Currently, there are no published reports of these small-molecule BTK inhibitors in clinical trials of autoimmune/inflammatory diseases. In contrast, a prodrug version of the SYK inhibitor, R406, is in Phase II clinical trials for rheumatoid arthritis.²⁹

The LFA-1 small-molecule antagonists, BMS 587101 and BIRT 377, potently blocked LFA-1/ICAM 1 adhesion in the EPIC assay. In a recent report, BMS 587101 blocked T cell–HUVEC (human umbilical vein endothelial cell) adhesion.¹⁵ Similar to the principles of monitoring LFA-1/ICAM-1 adhesion in the EPIC assay, T cells and HUVECs were stimulated with phorbol myristate acetate to increase LFA-1 avidity and ICAM-1 expression, respectively. BMS 587101 inhibited cell–cell adhesion with an IC_{50} of 20 nM and is consistent with our data (EPIC IC_{50} 23 nM; **Fig. 6B**). Furthermore, BMS 587101 showed efficacy in rodent models of arthritis.¹⁵ However, clinical trials to study BMS 587101 treatment in patients with moderate to severe psoriasis were terminated. BIRT 377 blocks LFA-1/ICAM-1 association by preventing upregulation of LFA-1 to its high-affinity conformation—a prerequisite for cell–cell adhesion.²⁶ BIRT 377 is reported to inhibit LFA-1/

ICAM-1 association in in vitro assays with a K_d of 26 nM and in cell-based adhesion assays in the low-micromolar range.³⁰ In our cell-based EPIC assay, the IC_{50} for BIRT 377 was 332 nM (Fig. 3C). Collectively, the EPIC assay platform can identify inhibitors that target upstream pathways of B cell activation (such as BTK) as well as downstream effectors proximal to LFA-1/ICAM-1 association and cast a wide net.

From a biology perspective, we wanted to examine the application of each platform to B cell activation that was elicited by a signaling pathway independent of BCR. B cell activation can be elicited on activation of the CD40 receptor. Importantly, CD40R signaling is expected to coalesce at the level of BTK (Fig. 1). The EPIC platform elicited a CD40R-dependent response; however, the FLIPR assay did not, and this was a major distinguishing attribute between the two platforms. An interesting observation of the EPIC assay was the profile of the kinetic trace for each method of activating B cell activation. There was a clear difference in the kinetic trace profile of the anti-IgM versus mega CD40L. Anti-IgM elicited a maximum response (LFA-1/ICAM-1 adhesion) within the first 30 min. In contrast, mega CD40L elicited a maximum response at the end of the kinetic read (120 min). These data may indicate that distinct signaling pathways are elicited on anti-IgM- or mega CD40L-mediated LFA1/ICAM-1 adhesion. Alternatively, the difference in kinetic profile may relate to the proclivity of the anti-IgM or mega CD40L to stay bound to the respective receptor. Given the robust and rapid nature of BCR activation, the desensitization and return of BCR signaling to basal levels may be tightly regulated, rapid, and distinct when compared to CD40R activation. Interestingly, coapplication of anti-IgM plus mega CD40L potentiated LFA-1/ICAM-1 association above that of anti-IgM or mega CD40L alone. This would suggest that CD40R and BCR signaling pathways are distinct in RL cells. Importantly, neither treatment of anti-IgM or mega CD40L alone maximized LFA-1/ICAM-1 association, enabling the identification of compounds that may potentiate LFA-1/ICAM-1 association above that of anti-IgM or mega CD40L.

Based on the signaling pathways illustrated in Figure 1, we validated that AVL-292 would inhibit CD40R-mediated LFA-1/ICAM-1 association. AVL-292 and its derivative attenuated anti-IgM and anti-IgM + mega CD40L-mediated LFA-1/ICAM-1 adhesion at 10 μ M. Also, AVL-292 and its derivative gave distinct EPIC profiles in response to mega CD40L B cell activation during the course of the kinetic read. For example, both AVL-292 and its derivative equally inhibited anti-IgM response at 30 min; however, there is a clear distinction in the inhibitory propensity of each compound post 30-min mega CD40L treatment. This distinction was not captured in the FLIPR assay or when using a set time point in the EPIC, and perhaps it illustrates the value of the EPIC kinetic trace. It is unclear why the AVL-292 derivative is less efficacious at inhibiting mega CD40L versus anti-IgM mediated EPIC response post 30-min application. We speculate that the

on/off rate of the AVL-292 derivative versus AVL-292 may differ in cells stimulated with mega CD40L; however, further investigation is needed.

From a phenotypic perspective, the EPIC B cell activation assay is designed to identify inhibitors that target known proteins as well as other novel mechanisms of action. However, deconvoluting the hits post HTS poses a challenge. Perhaps an attribute of the EPIC assay that distinguishes it from the FLIPR cell-based assay is the kinetic profile of a given compound. For example, it may be possible to further group HTS hits based on their kinetic trace profile. From a therapeutic standpoint, examining kinetic profiles of B cell inhibitor drugs with desirable and undesirable properties may provide a “profile signature” that can be used to group inhibitors of B cell activation post screening. However, suitable follow-up assays should be in place to validate this hypothesis. Profiling drugs for a “signature” or “fingerprint” has been addressed in the high-content-imaging arena. For example, Anne Carpenter’s lab at the Broad Institute used image-based profiling of a myriad of cellular morphological responses in response to small-molecular treatment using CellProfiler software. Both the phenotypic image-based and the EPIC-based approaches may provide useful insights for predicting a compound’s mechanism of action in a target-agnostic paradigm.

In summary, both the EPIC LFA-1/ICAM-1 adhesion assay and the FLIPR Ca^{2+} assay can identify inhibitors of B cell activation. The FLIPR-based assay is more amenable to ultra-HTS compared to the EPIC assay; however, given that the readout of the EPIC assay is further downstream than the FLIPR-based Ca^{2+} release, we anticipate that the EPIC assay will identify more inhibitors with differing mechanisms of action. Moreover, the EPIC assay appears more sensitive to different methods of activating B cells (i.e., mega-CD40L/anti-IgM) when compared to the FLIPR assay. Both phenotypic assays are complementary to each other, and the choice of platform will largely depend on the biological question to be addressed.

Acknowledgments

We acknowledge Nidhi Arora for thoughtful discussions.

Declaration of Conflicting Interests

The authors declared no potential conflicts of interest with respect to the research, authorship, and/or publication of this article.

Funding

The authors received no financial support for the research, authorship, and/or publication of this article.

References

1. Di Paolo, J. A.; Huang, T.; Balazs, M.; et al. Specific Btk Inhibition Suppresses B Cell- and Myeloid Cell-Mediated Arthritis. *Nat. Chem. Biol.* **2011**, *7*, 41–50.

2. Li, G.; Lai, F.; Fang, Y. Modulating Cell-Cell Communication with a High-Throughput Label-Free Cell Assay. *J. Lab. Autom.* **2012**, *17*, 6–15.
3. Armitage, R. J.; Fanslow, W. C.; Strockbine, L.; et al. Molecular and Biological Characterization of a Murine Ligand for CD40. *Nature*. **1992**, *357*, 80–82.
4. Elgueta, R.; Benson, M. J.; de Vries, V. C.; et al. Molecular Mechanism and Function of CD40/CD40L Engagement in the Immune System. *Immunol. Rev.* **2009**, *229*, 152–172.
5. Lipsky, P. E. Systemic Lupus Erythematosus: An Autoimmune Disease of B Cell Hyperactivity. *Nat. Immunol.* **2001**, *2*, 764–766.
6. Kotzin, B. L. The Role of B Cells in the Pathogenesis of Rheumatoid Arthritis. *J. Rheumatol.* **2005**, *73* (Suppl.), 14–18; discussion, 29–30.
7. Morrogh, L. M.; Hinshelwood, S.; Costello, P.; et al. The SH3 Domain of Bruton's Tyrosine Kinase Displays Altered Ligand Binding Properties When Auto-Phosphorylated In Vitro. *Eur. J. Immunol.* **1999**, *29*, 2269–2279.
8. Nore, B. F.; Vargas, L.; Mohamed, A. J.; et al. Redistribution of Bruton's Tyrosine Kinase by Activation of Phosphatidylinositol 3-Kinase and Rho-Family GTPases. *Eur. J. Immunol.* **2000**, *30*, 145–154.
9. Ghandour, H.; Cullere, X.; Alvarez, A.; et al. Essential Role for Rap1 GTPase and Its Guanine Exchange Factor CalDAG-GEFI in LFA-1 but Not VLA-4 Integrin Mediated Human T-Cell Adhesion. *Blood*. **2007**, *110*, 3682–3690.
10. Carrasco, Y. R.; Fleire, S. J.; Cameron, T.; et al. LFA-1/ICAM-1 Interaction Lowers the Threshold of B Cell Activation by Facilitating B Cell Adhesion and Synapse Formation. *Immunity*. **2004**, *20*, 589–599.
11. Springer, T. A. Adhesion Receptors of the Immune System. *Nature*. **1990**, *346*, 425–434.
12. Hantschel, O.; Rix, U.; Schmidt, U.; et al. The Btk Tyrosine Kinase Is a Major Target of the Bcr-Abl Inhibitor Dasatinib. *Proc. Natl. Acad. Sci. USA*. **2007**, *104*, 13283–13288.
13. McCaig, A. M.; Cosimo, E.; Leach, M. T.; et al. Dasatinib Inhibits B Cell Receptor Signalling in Chronic Lymphocytic Leukaemia but Novel Combination Approaches Are Required to Overcome Additional Pro-Survival Microenvironmental Signals. *Br. J. Haematol.* **2011**, *153*, 199–211.
14. Evans, E. K.; Tester, R.; Aslanian, S.; et al. Inhibition of Btk with CC-292 Provides Early Pharmacodynamic Assessment of Activity in Mice and Humans. *J. Pharmacol. Exp. Ther.* **2013**, *346*, 219–228.
15. Suchard, S. J.; Stetsko, D. K.; Davis, P. M.; et al. An LFA-1 (alphaLbeta2) Small-Molecule Antagonist Reduces Inflammation and Joint Destruction in Murine Models of Arthritis. *J. Immunol.* **2010**, *184*, 3917–3926.
16. Kuglstatter, A.; Wong, A.; Tsing, S.; et al. Insights into the Conformational Flexibility of Bruton's Tyrosine Kinase from Multiple Ligand Complex Structures. *Protein Sci.* **2011**, *20*, 428–436.
17. Douhan, J., 3rd; Miyashiro, J. S.; Zhou, X.; et al. A FLIPR-Based Assay to Assess Potency and Selectivity of Inhibitors of the TEC Family Kinases Btk and Itk. *Assay Drug Dev. Technol.* **2007**, *5*, 751–758.
18. Braselmann, S.; Taylor, V.; Zhao, H.; et al. R406, an Orally Available Spleen Tyrosine Kinase Inhibitor Blocks fc Receptor Signaling and Reduces Immune Complex-Mediated Inflammation. *J. Pharmacol. Exp. Ther.* **2006**, *319*, 998–1008.
19. Norman, P. A Novel Syk Kinase Inhibitor Suitable for Inhalation: R-343(?)—WO-2009031011. *Expert Opin. Ther. Pat.* **2009**, *19*, 1469–1472.
20. Lombardo, L. J.; Lee, F. Y.; Chen, P.; et al. Discovery of N-(2-Chloro-6-Methyl-Phenyl)-2-(6-(4-(2-Hydroxyethyl)-Piperazin-1-Yl)-2-Methylpyrimidin-4-Ylamino)Thiazole-5-Carboxamide (BMS-354825), a Dual Src/Abl Kinase Inhibitor with Potent Antitumor Activity in Preclinical Assays. *J. Med. Chem.* **2004**, *47*, 6658–6661.
21. Honigberg, L. A.; Smith, A. M.; Sirisawad, M.; et al. The Bruton Tyrosine Kinase Inhibitor PCI-32765 Blocks B-Cell Activation and Is Efficacious in Models of Autoimmune Disease and B-Cell Malignancy. *Proc. Natl. Acad. Sci. USA*. **2010**, *107*, 13075–13080.
22. Xu, D.; Kim, Y.; Postelnek, J.; et al. RN486, a Selective Bruton's Tyrosine Kinase Inhibitor, Abrogates Immune Hypersensitivity Responses and Arthritis in Rodents. *J. Pharmacol. Exp. Ther.* **2012**, *341*, 90–103.
23. Dinh, M.; Grunberger, D.; Ho, H.; et al. Activation Mechanism and Steady State Kinetics of Bruton's Tyrosine Kinase. *J. Biol. Chem.* **2007**, *282*, 8768–8776.
24. Barrett, T. B.; Shu, G.; Clark, E. A. CD40 Signaling Activates CD11a/CD18 (LFA-1)-Mediated Adhesion in B Cells. *J. Immunol.* **1991**, *146*, 1722–1729.
25. Sigal, A.; Bleijs, D. A.; Grabovsky, V.; et al. The LFA-1 Integrin Supports Rolling Adhesions on ICAM-1 under Physiological Shear Flow in a Permissive Cellular Environment. *J. Immunol.* **2000**, *165*, 442–452.
26. Woska, J. R., Jr.; Shih, D.; Taqueti, V. R.; et al. A Small-Molecule Antagonist of LFA-1 Blocks a Conformational Change Important for LFA-1 Function. *J. Leukoc. Biol.* **2001**, *70*, 329–334.
27. Jeon, H. K.; Ahn, J. H.; Choe, J.; et al. Anti-IgM Induces Up-regulation and Tyrosine-Phosphorylation of Heterogeneous Nuclear Ribonucleoprotein K Proteins (hnRNP K) in a Ramos B Cell Line. *Immunol. Lett.* **2005**, *98*, 303–310.
28. Burger, J. A. Bruton's Tyrosine Kinase (BTK) Inhibitors in Clinical Trials. *Curr. Hematol. Malig. Rep.* **2014**, *9*, 44–49.
29. Weinblatt, M. E.; Kavanaugh, A.; Genovese, M. C.; et al. An Oral Spleen Tyrosine Kinase (Syk) Inhibitor for Rheumatoid Arthritis. *N. Engl. J. Med.* **2010**, *363*, 1303–1312.
30. Kelly, T. A.; Jeanfavre, D. D.; McNeil, D. W.; et al. Cutting Edge: A Small Molecule Antagonist of LFA-1-Mediated Cell Adhesion. *J. Immunol.* **1999**, *163*, 5173–5177.